



1       **Overview: Cascading spatial, seasonal, and temporal effects of permafrost thaw on**  
2       **streamflow in changing nested Arctic catchments**

3       Alexa M. Hinzman<sup>1</sup>, Ylva Sjöberg<sup>2,3</sup>, Steve W. Lyon<sup>4</sup>, Wouter R. Berghuijs<sup>1</sup>, Ype van der  
4       Velde<sup>1</sup>

5             1 Department of Earth and Science, Vrije Universiteit Amsterdam, Amsterdam, Netherlands

6             2 Department of Geoscience and Natural Resource Management, University of Copenhagen,  
7       Copenhagen, Denmark

8             3 Department of Ecology and Environmental Science, Umeå University, Umeå, Sweden

9             4 School of Environment and Natural Resources, Ohio State University, Ohio, United States  
10       of America

11       Corresponding Author: Alexa Hinzman, [a.m.h.hinzman@vu.nl](mailto:a.m.h.hinzman@vu.nl)

12       Abstract:

13       In the Arctic, the thawing of permafrost affects how catchments store and release water.  
14       However, the effects of thawing on the hydrological response remain poorly documented. In  
15       addition, it remains unclear how the effects of a thawing landscape will propagate through  
16       nested catchments. Here we investigate 10 nested catchments within the Yukon basin (Alaska  
17       and Canada) to study how permafrost thaw impacts catchments' streamflow seasonality and  
18       storage-discharge relationships, and how these effects cascade through the nested catchments,  
19       from headwaters to downstream. Our results indicate that upstream catchments, characterized by  
20       continuous permafrost, have stronger streamflow seasonality and that these catchments also  
21       exhibit the most nonlinear storage-discharge relationships. Larger catchments downstream  
22       sustain year-round streamflow with baseflow continuing during winter. Since the 1950s flow  
23       regimes have become increasingly seasonal in the upstream catchments, with an earlier and  
24       more abrupt freshet, whereas further downstream flow seasonality has remained stable. Across  
25       the Yukon, storage-discharge relationships for 9 out of 10 sub-catchments have become  
26       increasingly nonlinear over time, with the biggest change occurring in the largest downstream  
27       catchments. In smaller catchments, each season has distinct recession characteristics, but those  
28       seasonal differences are not apparent further downstream. Upstream catchments are strongly  
29       influenced by localized change, whereas downstream catchments receive the effects of many  
30       different localized upstream impacts, making it difficult to detect a singular cause of change.  
31       Seasonal and long-term shifts in storage-discharge relationships are typically not accounted for  
32       by hydrological models and make accurate streamflow predictions more difficult. These shifts  
33       highlight how the changing landscape of the Arctic has far-reaching hydrological  
34       consequences.



35        **1 Introduction**

36                The Arctic is warming at a faster rate than any other region in the world (Rantanen et al.,  
37                2022). The Arctic is heterogeneous, as polar and subpolar zones feature many biomes, various  
38                habitats, and diverse soil compositions. The arctic desert, tundra, taiga, and boreal forest zones  
39                are all connected by the hydrologic continuum, by water moving from soil to headwater streams  
40                in uplands, through lowlands, and eventually to high-order streams in coastal areas. (McKenzie  
41                et al., 2021a).

42                Permafrost is a ubiquitous feature of the Arctic. Not considering the impact of  
43                permafrost on Arctic rivers will give an incomplete understanding of how Arctic catchments  
44                behave, especially now that the permafrost is thawing. Changes in catchment hydrology caused  
45                by permafrost thaw can lead to changes in groundwater flow, biodiversity, and the development  
46                of lakes and unfrozen conduits for groundwater (taliks) (Tananaev and Lotsari, 2022). Thawing  
47                catchments in the Arctic have undergone changes such as lowering of the permafrost table,  
48                marked subsidence of the ground surface, increased active layer thickness, and the expansion  
49                and connection of previously isolated taliks (Jin et al., 2022). In addition, in the Arctic, where  
50                direct human-ecosystem interactions are limited, land-cover change determined by climate  
51                change and permafrost thaw influences streamflow more than human-induced landcover change  
52                (Frey and McClelland, 2009).

53                Arctic hydrologic responses to climate warming vary between seasons (Wang et al.,  
54                2021). Firstly, the thawing permafrost can increase the hydrologic connectivity between aquifers  
55                and surface waters (Lamontagne-Hallé et al., 2018; Chiasson-Poirier et al., 2020). This can lead  
56                to increased surface-subsurface water exchange. Secondly, a thicker active layer can contribute  
57                to the melting of excess ground ice but also allows soils to store more water. This can increase  
58                streamflow in winter due to the development of the supra-permafrost aquifers allowing for  
59                groundwater flow below the seasonal frost layer (Lyon and Destouni, 2010; Wellman et al.,  
60                2013; Walvoord and Striegl, 2007a; Walvoord et al., 2019). Finally, a longer thaw season can  
61                contribute to the thickening of the active layer, which in turn delays the active layer freeze-up



62 and will also contribute to increased winter river runoff (Sjöberg et al., 2021). Also, the  
63 percentage of permafrost coverage will cause different hydrologic responses. For example, in  
64 catchments with higher permafrost presence, more water leaves the catchment as discharge  
65 while in catchments with less permafrost coverage, there is water loss in the form of  
66 evapotranspiration and infiltration into deeper groundwater flow paths (Koch et al., 2022). These  
67 impacts are heavily intertwined and therefore make it hard to isolate singular changes. (Asano et  
68 al., 2020; Karlsen et al., 2016; Lyon et al., 2012)

69 The impacts of permafrost thaw on catchment hydrology are widely variable throughout  
70 the Arctic and the temporal rate of permafrost degradation also differs substantially between  
71 locations (Obu et al., 2019; Sergeant et al., 2021). If the climate warms, 0.1°C in 10 years, a  
72 trend seen in (Bekryaev et al., 2010) which does not include the current polar amplification  
73 occurring, catchments with mean annual air temperature around 0°C will be affected more than  
74 catchments with a mean annual air temperature of -5°C. Effectively, those catchments situated  
75 on that temperature threshold will be unable to re-freeze previously thawed permafrost in winter,  
76 exacerbating the thawing rates of permafrost while catchments with lower mean annual air  
77 temperatures have thicker active layers in summer but refreeze completely in winter (Åkerman  
78 and Johansson, 2008; Cooper et al., 2022).

79 Recession analysis uses streamflow records to provide insight into groundwater  
80 movement at the catchment scale. Traditionally, recession analysis quantifies baseflow  
81 dynamics, and the catchment water balance by inferencing the unconfined aquifer storage and  
82 release relationship and has successfully represented the lateral redistribution of groundwater in  
83 land surface systems (Troch et al., 2013). Relating the changes in subsurface groundwater flow  
84 to changes in surface discharge has been a method of investigating the catchment's storage-  
85 discharge relationship to the change in climate. In permafrost-laden catchments, recession  
86 analysis has been used in a round-about way to evaluate the health of the permafrost (e.g., if  
87 there is an increase in active layer thickness, the amount of groundwater that can be stored in a  
88 catchment changes which can influence flow paths in a catchment and therefore be detected in



89 the recession analysis). It can illustrate permafrost thaw trends by making similar inferences to  
90 the catchment's storage dynamics, such as the active layer thickening and the changing  
91 groundwater flow (Hinzman et al., 2020, 2022).

92 Previous studies (Lyon et al., 2009; Brutsaert and Hiyama, 2012) have tested if an  
93 increased active layer thickness will lead to an increase in the recession curve slope. Recent  
94 work by Sergeant et al. (2021) echoed knowledge of the complexity of Arctic systems and found  
95 a dominant decrease in the recession curve intercept (i.e., the rate of discharge decline at a  
96 discharge of 1mm/d during a recession, indicating an increase in baseflow) after examining over  
97 300 Arctic catchments from 1970 to 2000. Camporese et al. (2014), Cooper et al. (2022), and  
98 Sergeant et al. (2021) used the nonlinear relationships between saturated soil thickness and  
99 average baseflow to infer changes in the active layer thickness and found that the growth rate of  
100 the active layer has been accelerating in the last 20 years. Clearly, there are many ways how  
101 surface and subsurface processes affect each other. For that reason, the relationship between  
102 streamflow and storage does not yet have a concise explanation. In addition, due to the  
103 heterogeneous nature of the Arctic, dissimilar results should be expected.

104 While there has been ample research showing a change in the recession curve slope as  
105 permafrost degrades (Sjöberg et al., 2013; Bogaart et al., 2016; Hinzman et al., 2022), the  
106 question remains if changes in catchment streamflow are observable at all spatial scales or if the  
107 observed change diminishes at larger spatial scales. This is a crucial question because most  
108 streamflow of the larger rivers in the Arctic is measured with goals to estimate water and solute  
109 loads to the Arctic Ocean, but these large river systems are potentially less informative as  
110 indicators of permafrost change.

111 Here we study the effects of permafrost thaw on spatial differences, seasonal changes,  
112 and long-term shifts of streamflow seasonality and storage-discharge relationships in the Arctic.  
113 We focus on how these changes vary across nested catchments with spatial scale and how any  
114 effects of thawing may propagate downstream. This helps to understand how the effects of  
115 permafrost thaw on streamflow vary across spatial scales.



116

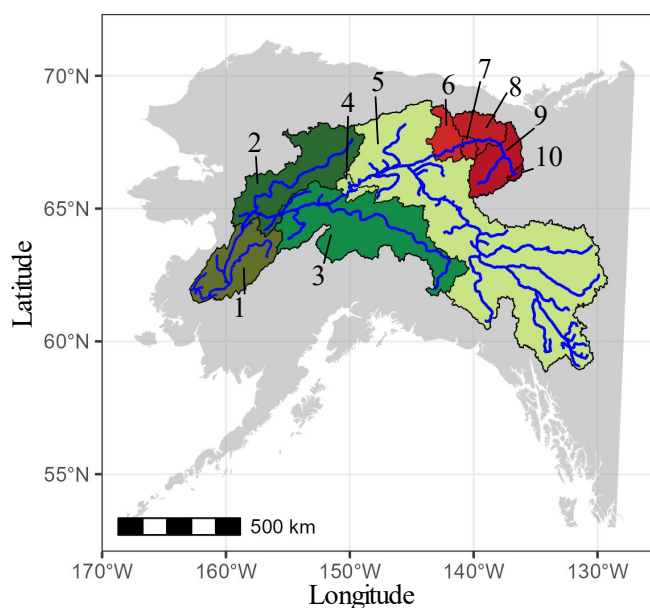
## 117 2 Methods

### 118 2.1 The Yukon Basin

119 We used data from 10 nested catchments from the Yukon basin in Alaska and Canada.

120 These catchments have a wide range of sizes as they cover the relatively smaller upstream

121 catchments, up to almost the entire basin near the mouth of the river (Figure 1; Table 1).



122

123 **Figure 1.** Outline of catchments, the blue lines indicate the river network, the smallest  
124 catchments are red and the rivers flow into the next larger catchment which changes to green.  
125 The catchments are numbered and correspond to Table 1.

126 We downloaded daily discharge data from the Global Runoff Data Centre (GRDC).

127 Monitoring for three catchments started in the 1950s, three in the 1960s, and three in the 1970s

128 with the latest catchment record starting in the 1980s. Four catchments have their data record

129 continue into the 21<sup>st</sup> century. Pilot Station has the longest dataset with 46 years, followed by

130 Steven Village with a dataset of 45 years. The exact date range and length of the record can be

131 found in Table 1.

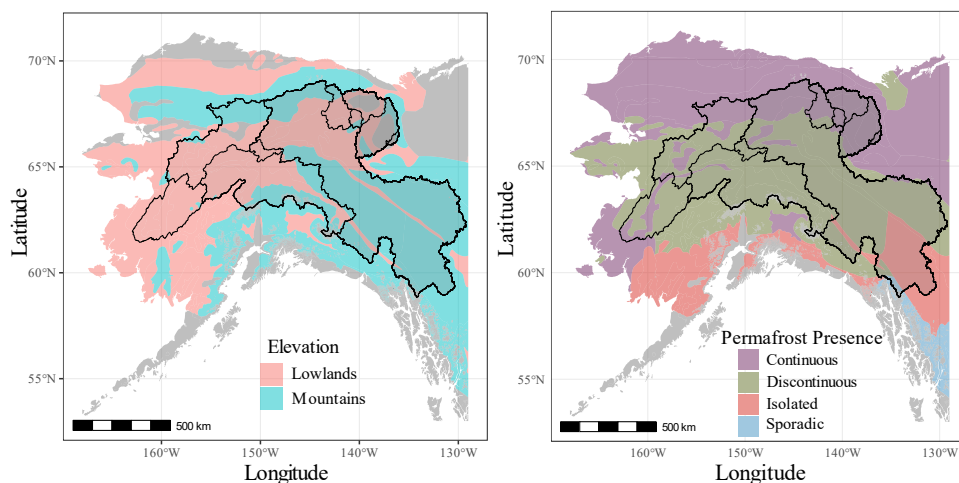


132 Meteorological data, such as precipitation and potential evapotranspiration, were  
 133 obtained from the Global Historical Climatology Network Daily (GHCN - Daily) dataset hosted  
 134 by the National Centers of Environmental Information (NCEI). In cases of missing data, we used  
 135 precipitation and potential evapotranspiration data from the gridded ERA5 dataset (Muñoz  
 136 Sabater, 2019, 2021).

137 **Table 1.** Information on 10 catchments used in this study.

Catchment Name (#)	River	Period	Lat (°)	Long (°)	Area (km <sup>2</sup> )	Missing Data
Pilot Station (1)	Yukon	1975-2020 (46)	61.9337	-162.8829	831390	18.4%
Kaltag (2)	Yukon	1956-1966 (11)	64.3271	-158.7219	766640	0.0%
Ruby (3)	Yukon	1956-1978 (23)	64.7405	-155.4919	670810	4.8%
Rampart (4)	Yukon	1956-1967 (12)	65.5065	-150.1734	516446	17.2%
Stevens Village (5)	Yukon	1976-2020 (45)	65.8751	-149.7203	508417	11.5%
Fort Yukon (6)	Porcupine	1964-1979 (16)	66.9903	-143.1404	76405	33.7%
International Boundary (7)	Porcupine	1987-2019 (33)	67.4239	-140.8938	59829	15.6%
Old Crow (8)	Porcupine	1961-1995 (35)	67.5639	-139.8833	55400	31.3%
Bell River (9)	Porcupine	1964-1995 (32)	67.4403	-137.7836	36000	44.5%
Dempster Highway Bridge (10)	Eagle	1978-2017 (40)	66.4417	-136.7083	1720	60.6%

138  
 139 We determined topography and permafrost presence by using the Circum-Arctic Map of  
 140 Permafrost and Ground-Ice Conditions dataset (Brown et al., 2002) from the National Snow and  
 141 Ice Data Center (NSIDC). The largest catchments are flatter, with alpine conditions from the  
 142 south consisting of the Alaska Range, and the Kuskokwim Mountains with moderate Arctic  
 143 conditions. The smaller catchments are further North, in a mix of alpine regions (Brooks Range  
 144 and Ogilvie Mountains) and lowland regions and moreover colder climate conditions (Figure  
 145 2a). Lowlands are defined by (Brown et al., 2002) as intra- and intermontane depressions and  
 146 terrains characterized by thick overburden cover (5-10m). While the uplands included  
 147 mountains, highlands ridges, and plateaus characterized by a thick overburden cover (>5m) or  
 148 exposed bedrock. We determined that during 2002, (when the Circum-Arctic map was first  
 149 published), the smaller, more Northern catchments were in a continuous permafrost region while  
 150 the downstream catchments had greater sections that encompass discontinuous and sporadic  
 151 permafrost regions (Figure 2b).



152

153 **Figure 2.** Outline of catchments with topography (a) and side-by-side of permafrost  
154 presence (b).

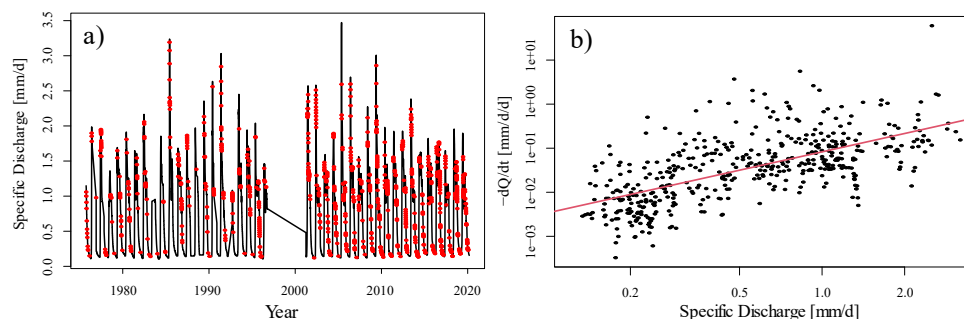
## 155 2.2 Streamflow and recession analysis

156 Discharge data were originally collected in cubic meters per second. We convert these data  
157 into specific discharge (i.e., mm/d) to allow more direct comparison between the catchments of  
158 strongly varying sizes. In addition, we calculate ratios of average monthly discharge to the  
159 average annual discharge (i.e., Pardé coefficients), first utilized by Maurice Pardé in 1933 and  
160 still used by hydrologists today to allow direct comparison of the streamflow seasonality  
161 between catchments (Curran and Biles, 2021; Poschod et al., 2020).

162 Many studies have expanded on Brutsaert and Nieber's (1977) work on recession analysis  
163 and Kirchner's (2009) work on Arctic catchments to further the understanding of permafrost's  
164 control of the catchment's response (Karlsen et al., 2019; Ploum et al., 2019; Sergeant et al.,  
165 2021). The basic recession curve analysis used in this study follows the method first explained in  
166 Hinzman et al. (2020) and then expounded in Hinzman et al. (2022) A concise explanation is  
167 that while the hydrograph is reclining (Figure 3a), signifying no extra influence from  
168 meteorological factors, the rate of change in discharge ( $dQ$ , [mm/d/d]) over a change in time ( $dt$ ,  
169 [d]) can be equated to the discharge ( $Q$ , [mm/d]) and the sensitivity of discharge to change in  
170 groundwater storage ( $dQ/dS$ , [ $d^{-1}$ ]), which in turn is approximately a power function of the



171 discharge ( $Q$ ) (Eq.1). The resulting constants (Figure 3b),  $\alpha$  and  $\beta$  can be interpreted as the  
 172 intercept ( $\alpha$ , [ $\text{mm}^{1-\beta}\text{d}^{\beta-2}$ ]) and the slope ( $\beta$ , [-]) of the recession curve, as explained in (Kirchner,  
 173 2009).



174

175 **Figure 3.** Hydrograph (a) and recession curve (b) of Pilot Station, red dots in (a) indicate  
 176 recession points, which are then used in Figure 1b. The red line in (b) is the recession curve  
 177 slope ( $\beta$ ), which is obtained by a linear regression. The hydrograph (a) has a y-axis of the  
 178 specific discharge. Specific discharge is discharge divided by catchment area. The specific  
 179 discharge is seen in the x-axis of (b), and the y-axis is the change of specific discharge over the  
 180 change of time.

181 
$$\frac{dQ}{dt} = -Q \frac{dQ}{dS} \approx -\alpha Q^\beta \quad 1)$$

182 **2.3 Temporal change analysis**

183 Our paper focuses on changes in the catchments' streamflow dynamics, as seen in changes  
 184 in the specific discharge or changes in the slope of the recession curve, to be referred to in the  
 185 future as  $\beta$ . Previous studies on arctic recessions (Lyon et al., 2009; Sjöberg et al., 2013; Evans  
 186 et al., 2020; Lyon and Destouni, 2010), held  $\beta$  constant ( $\beta = 1$ ) and focused on the recession  
 187 intercept ( $\alpha$ ). Our focus on  $\beta$  is to characterize the amount of water moving through the  
 188 catchment and to better examine the non-linear or linear relationship between discharge and  
 189 groundwater storage. The length of the data collected is substantial for five catchments. They are  
 190 Pilot Station (46 years), Ruby (23 years), Stevens Village (45 years), International Boundary (33  
 191 years), and Bell River (32 years), (Table 1). These catchments were gauged during different time  
 192 periods, thus, for comparison the datasets were divided into halves (early and later years). This  
 193 allows for comparison of hydrological changes within the catchments themselves as well as





194 direct comparison of the catchments that do have overlapping time series. We characterize  
195 streamflow seasonality (as expressed by Pardé coefficients) and streamflow recession behavior  
196 (as expressed by  $\beta$ ) for both the earlier and later periods. There are significant gaps in data  
197 collection for the Bell River and Dempster Highway Bridge. Those gaps arise from no stream  
198 discharge monitoring rather than a technical malfunction in data collection equipment. Other  
199 data gaps come from reduced monitoring frequency, especially in the earlier times of data  
200 collection as well as natural events like extreme weather conditions or floods that disrupt the  
201 normal functioning of measurement stations.

202

### 203 **3 Results and discussion**

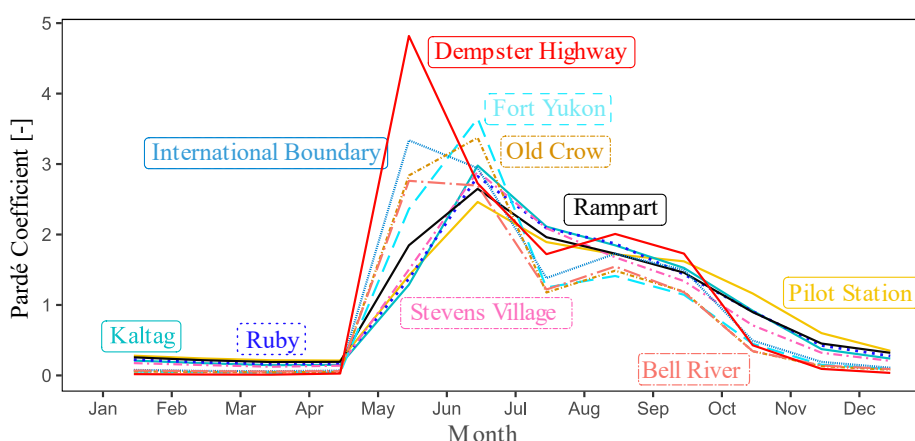
#### 204 **3.1 Spatial patterns in seasonality and streamflow recessions**

205 All catchments of the Yukon Basin have strongly seasonal streamflow regimes, but the  
206 degree of seasonality varies and is mediated by the catchment location within the Yukon River  
207 basin (Figure 4). Average monthly discharges for all catchments, as expressed by Pardé  
208 coefficients, indicate that smaller catchments that are located further upstream have relatively  
209 higher spring streamflows than the more downstream catchments. The smallest catchment,  
210 Dempster Highway Bridge (area = 1720 km<sup>2</sup>) has its highest mean monthly flow around May.  
211 This freshet is almost five times larger than the mean flow of this catchment. During July and  
212 August, flow rates show a slight increase caused by typically higher precipitation rates during  
213 summer than other periods of the year. From November through March flow rates become near-  
214 zero. The largest catchment (Pilot Station, area = 831,390 km<sup>2</sup>) has a more dampened highest  
215 mean monthly flow that also occurs later in the season. This peak flow is ~ 2.5 times the  
216 catchment's mean monthly flow rate and occurs around June. From thereon, flow reduces over  
217 summer, and low flows (Pardé coefficient ~0.25) persist also during the winter period up to the  
218 freshet. The other nested catchments have maximum seasonality patterns that fall between these  
219 two upstream and downstream end-member catchments. Overall, the Pardé coefficient indicates  
220 that larger catchments are less impacted by local factors throughout the year, resulting in more



221 consistent year-round streamflow. Curran and Biles (2021) analyzed Pardé coefficients for 253  
222 Alaskan catchments grouped by subclasses like winter temperature and basin elevation. The  
223 catchments they classified as driven by snowmelt or rainfall streamflow were comparable to the  
224 catchments in our study. Furthermore, their Pardé coefficients were similar, and their conclusion  
225 of shifting geographic seasonality echoed our own findings.

226



227

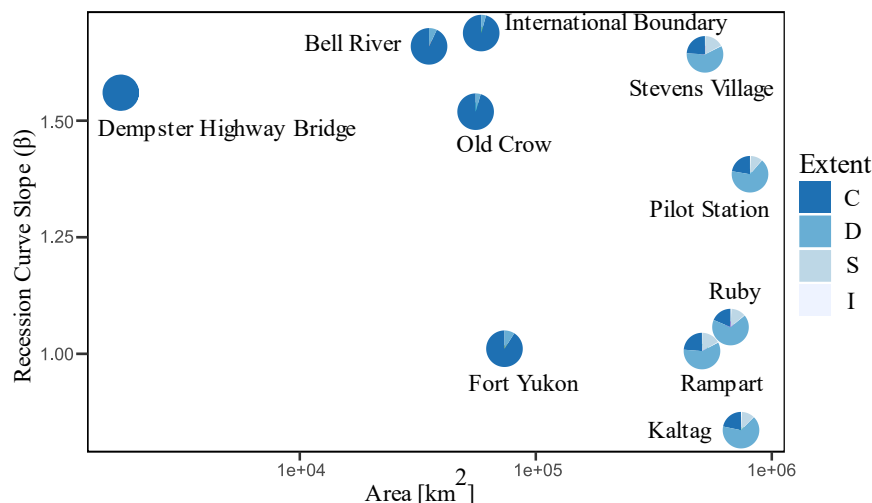
228 **Figure 4.** Seasonal flow regimes of the nested catchments within the Yukon basin.  
229 Comparison of Pardé coefficients, the catchments located in the North tend to have higher  
230 monthly Pardé coefficients compared to the catchments in the South, except during the winter  
231 months, when the northern catchments do not have any streamflow.

232

233 Streamflow recession behavior for all seasons over the whole times series, as  
234 characterized by the dimensionless recession slope  $\beta$ , is also mediated by the catchment's  
235 location within a basin (Figure 5). Smaller upstream catchments ( $<100,000 \text{ km}^2$ ) tend to have  
236 steeper recession curve slopes than the larger downstream catchments (Figure 5). Spatially, the  
237 smaller catchments have a higher percentage of continuous permafrost (Figure 5) as well as  
238 steeper slopes. Interestingly, steeper slopes correlate with greater changes in  $\beta$  was a result found  
239 in (Hinzman et al., 2022), which may explain the findings here. The catchments' permafrost  
240 becomes mostly discontinuous downstream of Stevens Village (area =  $508,417 \text{ km}^2$ ). In larger  
241 catchments ( $> 500,000 \text{ km}^2$ ) further downstream than Stevens Village,  $\beta$  decreases suddenly and  
242 there is a wider range of recession curve slopes (0.80-1.70), while upstream  $\beta$  appears relatively  
constant and high ( $\sim 1.5$ -1.7), with the exception of Fort Yukon ( $\beta = \sim 1.0$ ). This wide range of



243 recession curve slopes seen in the large catchments can be attributed to those catchments having  
244 different time periods of data collection.



245

246 **Figure 5.** Recession curve slopes vs area of catchments. Note that the period for which  
247 the recession curve slopes are determined may vary between stations (Table 1). The pie graphs  
248 indicate the percentage of different permafrost for each catchment during the early 2000s. C is  
249 continuous permafrost (90-100%), D is discontinuous permafrost (50-90%), S is sporadic  
250 permafrost (10-50%) and I is isolated permafrost (0-10%).

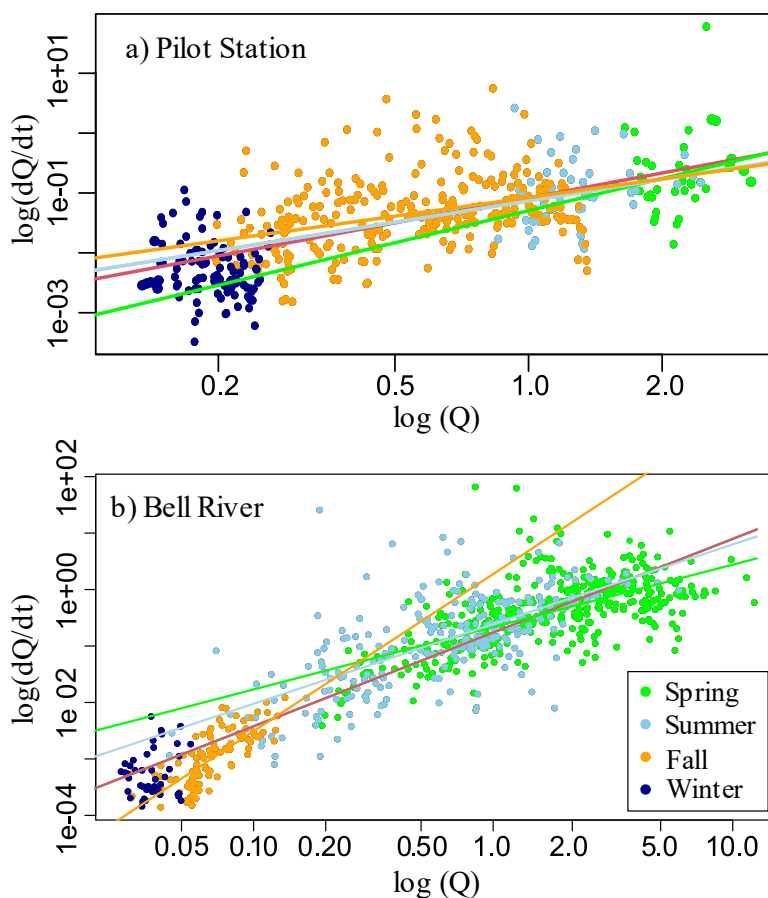
### 251 3.2 Seasonal shifts in recession behavior

252 The rate at which frozen ground thaws varies throughout the year, and the effects of that  
253 thawing (i.e. differences in active layer thickness, taliks that widen/open and narrow/close, and  
254 permafrost thawing from the bottom) can result in distinct recession curve slopes between  
255 seasons. Several studies have looked at seasonal effects of ground freeze-thaw processes on  
256 streamflow, (Ploum et al., 2019; Wang et al., 2020). We first illustrate these seasonal shifts by  
257 calculating recession curve slopes for spring, summer, and fall at Pilot Station and Bell River  
258 (Figure 6). While winter recession points were included in the graphs, the winter recession curve  
259 slope was not considered as many of the upstream catchments do not have winter recessions due  
260 to low or no streamflow (Figure 4). At Pilot Station (Figure 6a), the recession curve slope does  
261 not substantially vary throughout the seasons, except for spring. In spring, the  $\beta$ -value ( $\sim 1.8$ ) is  
262 higher than in the other seasons where  $\beta$  is  $\sim 1.0$ - $1.2$ . For the upstream catchment of Bell River



263 (Figure 6b), there are much stronger seasonal differences in recession curve slopes. Here, fall  
264 has the highest recession curve  $\beta$  ( $\sim 2.2$ ) whereas the slope is lowest during spring ( $\sim 0.78$ ). More  
265 generally, when we consider seasonal recession curve slopes across all catchments (Table 2), we  
266 find that downstream catchments tend to have lower fall recession curve slopes, whereas in  
267 upstream catchments the recession curve slope continues to increase from spring to fall. This  
268 shift from spring to fall, where the recession becomes more non-linear, indicates that as the  
269 seasons progress, streamflow responses become more sensitive to storage variations and thereby  
270 potentially harder to predict. This echoes our seasonal findings from an earlier paper focused on  
271 Swedish catchments (Hinzman et al., 2020) where the summer recession curve slope was greater  
272 than the spring recession curve slope but we also found that spring recession curve slopes were  
273 increasing at a more rapid rate the summer recession curve slopes.

274 These changes in seasonal behavior can be attributed to several factors. In the upstream  
275 catchments, the thawing active layer will allow for increasing subsurface flow, with spring  
276 having the shallowest thickness of the active layer and fall having the deepest thickness of the  
277 active layer, while in downstream catchments the thickness of the active layer can already be  
278 fluctuating within the areas of discontinuous permafrost, leading some areas to already have  
279 deep thickness of active layer as well as with streamflow of different seasons flowing from the  
280 upstream catchments creating a blend of spring, summer or fall discharge further obfuscating  
281 seasonal recessions. Increasing groundwater flow as found in studies from Lyon et al. (2010)  
282 and Walvoord and Striegl (2007) lead researchers to suggest that this increase leads to more  
283 non-linearity in streamflow response and the increased storage capacity lengthens timescales and  
284 leads to the increased blending of streamflow seasonalities (Wang et al., 2022; Curran and Biles,  
285 2021).



286

287

288

289

290

291

292

293

**Figure 6.** Pilot Station (a), and Below Bell River (b) recession curve with seasonal recession points. Red is the overall recession curve slope. Light green represents the recession curve slope and recession points that occurred in spring. Light blue represents the recession curve slope and recession points that occurred in summer. Orange represents the recession curve slope and recession points that occurred in fall. Dark blue represents recession points that occurred in winter. The y-axis is log of the change of discharge over the change in time, and the x-axis is the log of discharge.

294

**Table 2.** Recession Curve  $\beta$  results, stratified per season.

Catchment	Area (km <sup>2</sup> )	Overall $\beta$	Spring $\beta$	Summer $\beta$	Fall $\beta$
Pilot Station	831,390	1.38	1.78	1.19	1.03
Kaltag	766,640	0.833	NA	1.06	0.701
Ruby	670,810	1.06	NA	3.04	0.872
Rampart	516,446	1.01	3.27	2.83	0.967
Stevens Village	508,417	1.65	1.25	NA	1.61
Fort Yukon	76,405	1.01	0.942	1.12	NA
International Boundary	59,829	1.69	1.2	1.25	1.82
Old Crow	55,400	1.53	0.902	1.27	2.44



	Bell River	36,000	1.66	0.779	1.38	2.17
295	Dempster Highway Bridge	1,720	1.56	0.46	1.42	1.54

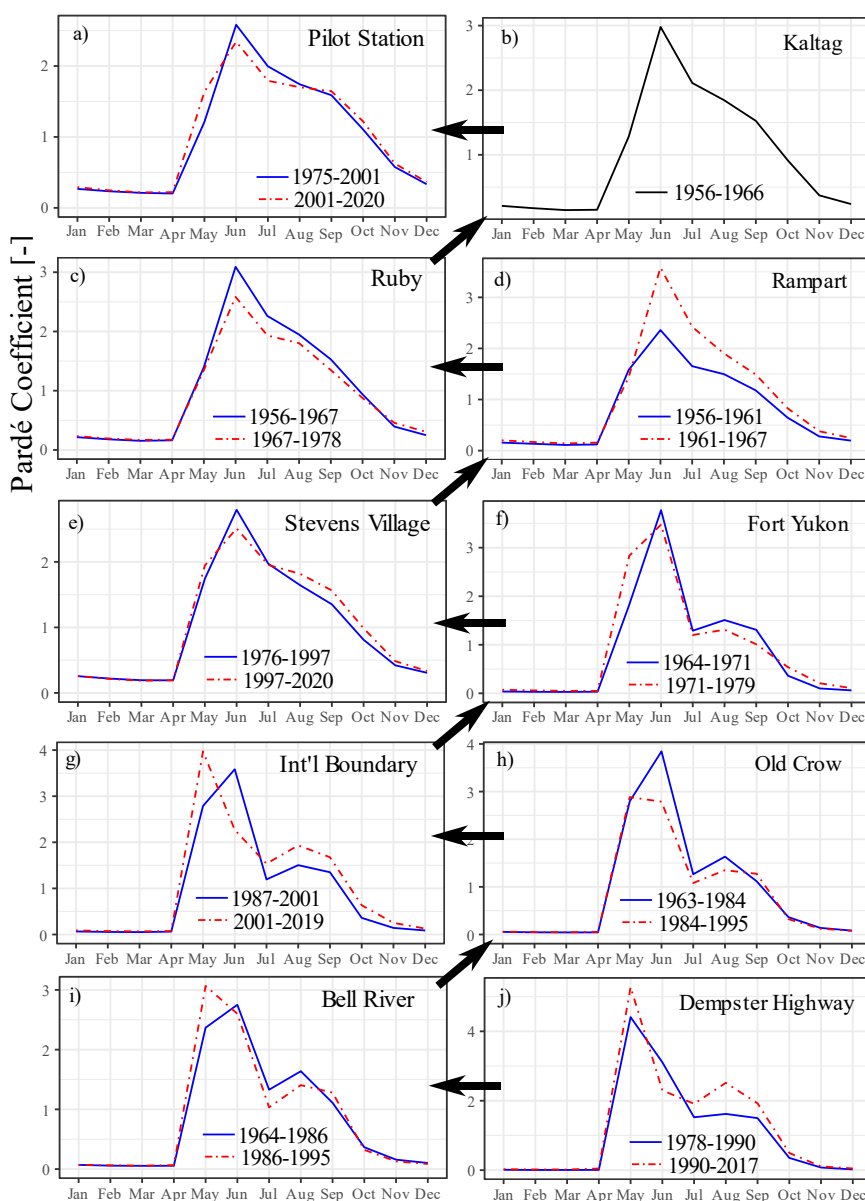
296 3.3 Temporal change in seasonality and recession behavior

297 The changes in the Arctic are not confined solely to seasonal patterns; rather, the  
298 warming of the Arctic instigates enduring shifts in hydrological behavior over the long term. For  
299 catchments where we could divide the dataset into an early and late period (both with >7 years  
300 of (near-) continuous data), we calculate monthly Pardé coefficients for the early and the late  
301 period, using the average discharge value for the entire dataset, thus allowing for a comparison  
302 temporally and seasonally.

303 In most catchments, streamflow seasonality appears to be changing over time (Figure 7),  
304 whereby the patterns of change vary according to the location within the basin. In the upstream  
305 stations, the spring discharge peak has shifted towards an earlier start (Figure 7f-7j), and this  
306 freshet has not consistently changed its magnitude compared to the older period. In these  
307 upstream catchments, streamflow has remained marginal during early winter (October-  
308 December) and near zero throughout the later winter months (January-March). Similarly, for  
309 almost all of the downstream catchments (Stevens Village and larger), the freshet has slightly  
310 shifted towards an earlier start, while spring peak flows have remained similar, except in  
311 Rampart and Ruby. For Rampart the change in Pardé coefficients suggests greater streamflow  
312 throughout the second period while Ruby has less streamflow during the second period. Another  
313 shift we observe in downstream catchments are increases in streamflow throughout late fall and  
314 early winter (Oct-Dec), as indicated by the larger Pardé coefficients. While downstream  
315 catchments have year-round streamflow, later winter months streamflow has remained constant  
316 over the years, which is consistent with no changes seen in the winter months of upstream  
317 catchments (Fig. 7a-7j). Moreover, the earlier start of the season is clear in the upstream, smaller  
318 catchments and less pronounced in downstream catchments. However, for downstream  
319 catchments impacts extend into the late fall and early winter periods. Downstream catchments  
320 interact with larger and typically deeper groundwater aquifers. The flow through these aquifers



321 has been shown to increase by permafrost thaw leading to larger baseflow and increasingly non-  
322 linear storage discharge relationships (Walvoord et al., 2012; Hinzman et al., 2020). Analyses of  
323 other basins, such as the Yana and Indigirka basins in Russia have shown shifting streamflows,  
324 with increasing streamflows into September, an increasing number of rivers not freezing in  
325 November or December, and earlier recorded freshet (Makarieva et al., 2019).





327 **Figure 7.** Changes in the average monthly streamflow of catchments. Blue solid lines  
 328 represent the earlier years of the dataset, and the red dotted line represents the later years of the  
 329 catchment, the length of each catchment’s record can be found in Table 1. The black arrows  
 330 indicate the directions of the catchment flow.

331 Across the Yukon, 9 out of 10 sub-catchments’ storage-discharge relationships have  
 332 become increasingly nonlinear as time progressed. These changes are often substantial, as for  
 333 example, Pilot Station shifts draining roughly linearly (early  $\beta = 0.93$ ) towards substantially  
 334 nonlinear (later  $\beta = 1.55$ ). For most of the other catchments,  $\beta$  has increased roughly 0.3-0.4. The  
 335 largest changes have occurred in the downstream catchments (most notably Pilot Station and  
 336 Rampart), whereas changes in the upstream catchments (e.g., Old Crow, Bell River, Dempster  
 337 Highway Bridge) tend to be of a smaller magnitude. Ruby and Rampart have large differences  
 338 between early and later periods (early  $\beta = 0.706$ , later  $\beta = 1.06$  and early  $\beta = 2.09$ , later  $\beta = 1.01$ ,  
 339 respectively), with the later  $\beta$  being almost identical to the overall  $\beta$ , which reflects there were  
 340 few recession points captured in earlier periods compared to later periods. Few recession points  
 341 in the earlier period may also cause larger uncertainty in the early  $\beta$  of Ruby and Rampart. Our  
 342 results of increased non-linearity in  $\beta$  differed from the work by Sergeant et al. (2021), who  
 343 found a decreasing recession curve  $\beta$  for a majority of their catchments. However, an  
 344 explanation for this difference could be in the length of the dataset, with Sergeant using data  
 345 from 1970-2000 and our study encompassed data from 1954-2020, an extra 40 years. Other  
 346 studies agree with our findings of increased  $\beta$  values (e.g., McKenzie et al., 2021b; Ploum et al.,  
 347 2019; Wang et al., 2022).

348 **Table 3.** Recession characteristics for early and later periods. 3.4 Nested catchments as  
 349 expenditures of missing data

Catchment	Area (km <sup>2</sup> )	Overall $\beta$	Period	Early $\beta$	Period	Later $\beta$
Pilot Station	831,390	1.38	1975-2001	0.93	2001-2020	1.55
Kaltag	766,640	0.833	1956-1961	NA	1961-1966	NA
Ruby	670,810	1.06	1956-1967	0.71	1967-1978	1.06
Rampart	516,446	1.01	1956-1961	2.09	1961-1967	1.01
Stevens Village	508,417	1.65	1976-1997	1.37	1997-2020	1.8
Fort Yukon	76,405	1.01	1964-1971	0.80	1971-1979	1.2
International Boundary	59,829	1.69	1987-2001	1.68	2001-2019	1.71
Old Crow	55,400	1.53	1963-1984	1.32	1984-1995	1.72
Bell River	36,000	1.66	1964-1986	1.49	1986-1995	1.77





Dempster Highway Bridge	1,720	1.56	1978-1990	1.36	1990-2017	1.69
----------------------------	-------	------	-----------	------	-----------	------

350 In cases of missing data, which is a common issue within the Yukon basin and the  
351 Arctic more broadly, our analysis of cascading spatial, seasonal, and temporal effects of  
352 permafrost thaw on streamflow may help to fill data gaps. There are clear patterns in upstream  
353 and downstream differences in seasonal flow patterns (Fig 4), recession characteristics (Fig. 5),  
354 and temporal shifts of these flow patterns and recession characteristics (Figs 7a-7j). This implies  
355 that in cases of missing data (either because a gauge is not operational or because there is no  
356 gauge at all), we can use the data of surrounding catchments to estimate flow seasonality,  
357 recession behavior, and temporal shifts of the ungauged catchment. The most representative  
358 donor catchments are not necessarily the closest in geographic location, but they are the ones  
359 that most closely resemble the catchment's location within the river network, and the associated  
360 permafrost conditions. Such information is readily available across the entire Yukon basin (or  
361 even the Arctic) and thereby allows for wide application.

362 Such estimates could not only provide estimates in space, but also provide estimates in  
363 time. For example, Pilot Station data collection started in 1975, in other words, it was an  
364 ungauged catchment before 1975 and therefore earlier streamflow and recession behavior are  
365 unknown. However, data from a nearby and representative station (Kaltag) goes back to 1956. It  
366 is very similar in size (a 7.8% area difference), in permafrost characteristics (22.4% and 21.8%  
367 of the catchments are covered in continuous permafrost, with 66.7% and 66.3% covered by  
368 discontinuous permafrost) and in the relative location within the catchment. Using the data from  
369 Kaltag to estimate catchment behavior during the earlier years of an ungauged Pilot Station  
370 would be beneficial in creating a longer time frame of which to document changes in the  
371 catchment.

372 Data from similar-sized catchments further supports the use of data from other  
373 catchments to create a more complete data record, because both Pardé coefficients and recession  
374 curve slope are comparable in similar sized catchments. For example, the Pardé coefficients and



375 the recession curve slopes of Pilot Station and Ruby are comparable over the period where data  
376 of the two catchments overlap for (i.e., earlier  $\beta_{PS} = 0.932$  and later  $\beta_{Ru} = 1.06$ ). In addition, the  
377 earlier period seasonal flow regime of Pilot Station (1975-2001) (the blue line in Fig. 7a) is  
378 almost identical to the later period seasonal flow regime of Ruby (1967-1978) (red line in Figure  
379 7c). Another example is International Boundary and Old Crow, which only differ by 7.5% in  
380 size. These catchments have near-identical recession behavior (when the overlapping time  
381 period is considered) with a recession slope for International Boundary (1987-2001) of  $\beta_{IB}$   
382  $= 1.68$ , and the later part of Old Crow (1984-1995) of  $\beta_{OC} = 1.72$ . Such transfer of data likely  
383 becomes increasingly reliable when catchment properties and the considered period better  
384 overlap. A study by Betterle and Botter (2021) found that nested catchments had less streamflow  
385 correlation than non-nested catchments that were more similar in area and geomorphic  
386 conditions, while we do not find similar findings in our nested catchments, it does lead credence  
387 that the dataset of similar catchments, nested or otherwise, can be used to create a more  
388 complete picture when data is not available.

#### 389 **4 Conclusion**

390 The thawing of permafrost affects how Arctic catchments store and release water, but the  
391 effects of thawing on hydrological response are poorly documented. These effects will vary  
392 according to the location in the catchment, but it also is unclear how the effects of a potentially  
393 thawing landscape will propagate through nested catchments. Here we investigated 10 nested  
394 catchments within the Yukon basin (Alaska and Canada) to study how permafrost thaw impacts  
395 catchments' streamflow seasonality and storage-discharge relationships, and how these effects  
396 cascade through nested catchments, from headwaters to downstream. Our results indicate that  
397 upstream catchments, characterized by continuous permafrost, mostly have stronger streamflow  
398 seasonality, and that these catchments also exhibit the most nonlinear storage-discharge  
399 relationships. Larger catchments downstream sustain year-round streamflow with baseflow  
400 continuing during winter. Since the 1950s flow regimes have become increasingly seasonal in  
401 the upstream catchments, with an earlier and more abrupt freshet, whereas further downstream



402 flow seasonality has remained stable. Across the Yukon, 9 out of 10 sub-catchments' storage-  
403 discharge relationships have become increasingly nonlinear over time, with the biggest change  
404 in the largest downstream catchments. In smaller catchments, each season has distinct recession  
405 characteristics, but those seasonal differences are not apparent further downstream. Upstream  
406 catchments are strongly influenced by localized change, whereas downstream catchments  
407 receive many different localized upstream impacts, making it difficult to detect a singular cause  
408 of the change. Seasonal and long-term shifts in storage-discharge nonlinearity are typically not  
409 accounted for by hydrological models and make accurate streamflow predictions with a  
410 changing climate and thawing permafrost more difficult. These shifts highlight how the  
411 changing landscape of the Arctic has far-reaching hydrological consequences.

412 Data availability:

413 The paper uses streamflow data obtained from the Global Runoff Data Centre (GRDC) The full  
414 dataset and documentation can be downloaded from:  
415 <https://portal.grdc.bafg.de/applications/public.html?publicuser=PublicUser#dataDownload/Home>  
416 [e](#)

417 The paper uses meteorological data obtained from the Global Historical Climatology Network  
418 Daily (GHCN - Daily) <https://www.ncdc.noaa.gov/cdo-web/> The full dataset and documentation  
419 can be downloaded from DOI:10.7289/V5D21VHZ

420 For missing meteorological data the paper used gridded ERA5 dataset.  
421 <https://cds.climate.copernicus.eu/cdsapp#!/dataset/reanalysis-era5-single-levels?tab=overview>  
422 The full dataset and documentation can be downloaded from: DOI: 10.24381/cds.adbb2d47

423 The paper used data from Circum-Arctic Map of Permafrost and Ground-Ice Conditions  
424 <https://nsidc.org/data/ggd318/versions/2> The shapefiles and documentation can be downloaded  
425 here: DOI: 10.7265/skbg-kf16

426 For River Shapes the paper used Global River Classification (GloRiC)  
427 <https://www.hydrosheds.org/products/gloric> The shapefiles and documentation can be  
428 downloaded here: DOI: 10.1088/1748-9326/aad8e9

429 Author contribution:

430 Alexa M. Hinzman: Conceptualization, Formal analysis, Data Curation, Writing - Original  
431 Draft, Visualization. Ylva Sjöberg: Writing - Review & Editing. Steve W. Lyon: Writing -  
432 Review & Editing. Wouter R. Berghuijs: Conceptualization, Writing - Review & Editing,  
433 Visualization. Ype van der Velde: Methodology, Writing - Review & Editing, Visualization,  
434 Supervision.

435 Declaration of interests:

436 At least one of the (co-)authors is a member of the editorial board of The Cryosphere.

437 Funding:



- 438 This work is part of the research program Netherlands Polar Programme with project  
439 number ALWPP.2016.014, which is financed by the Dutch Research Council (NWO).
- 440 **5 References**
- 441 Åkerman, H. J. and Johansson, M.: Thawing permafrost and thicker active layers in sub-arctic  
442 Sweden, *Permafr Periglac Process*, 19, 279–292, <https://doi.org/doi:10.1002/ppp.626>, 2008.
- 443 Asano, Y., Kawasaki, M., Saito, T., Haraguchi, R., Takatoku, K., Saiki, M., and Kimura, K.: An  
444 Increase in Specific Discharge With Catchment Area Implies That Bedrock Infiltration Feeds  
445 Large Rather Than Small Mountain Headwater Streams, *Water Resour Res*, 56,  
446 e2019WR025658, <https://doi.org/https://doi.org/10.1029/2019WR025658>, 2020.
- 447 Bekryaev, R. V., Polyakov, I. V., and Alexeev, V. A.: Role of Polar Amplification in Long-Term  
448 Surface Air Temperature Variations and Modern Arctic Warming, *Journal of Climate*, 23, 3888–  
449 3906, <https://doi.org/https://doi.org/10.1175/2010JCLI3297.1>, 2010.
- 450 Betterle, A. and Botter, G.: Does Catchment Nestedness Enhance Hydrological Similarity?,  
451 *Geophys Res Lett*, 48, e2021GL094148, <https://doi.org/https://doi.org/10.1029/2021GL094148>,  
452 2021.
- 453 Bogaart, P. W., Van Der Velde, Y., Lyon, S. W., and Dekker, S. C.: Streamflow recession  
454 patterns can help unravel the role of climate and humans in landscape co-evolution, *Hydrol*  
455 *Earth Syst Sci*, 20, 1413–1432, <https://doi.org/10.5194/hess-20-1413-2016>, 2016.
- 456 Brown, J., Ferrians, O., Heginbottom, J. A., and Melnikov, E.: Circum-Arctic Map of  
457 Permafrost and Ground-Ice Conditions, <https://doi.org/10.7265/skbg-kf16>, 2002.
- 458 Brutsaert, W. and Hiyama, T.: The determination of permafrost thawing trends from long-term  
459 streamflow measurements with an application in eastern Siberia, 22110 pp.,  
460 <https://doi.org/10.1029/2012JD018344>, 2012.
- 461 Brutsaert, W. and Nieber, J. L.: Regionalized drought flow hydrographs from a mature glaciated  
462 plateau, *Water Resour Res*, 13, 637–643, <https://doi.org/10.1029/WR013i003p00637>, 1977.
- 463 Camporese, M., Penna, D., Borga, M., and Paniconi, C.: A field and modeling study of nonlinear  
464 storage-discharge dynamics for an Alpine headwater catchment, *Water Resour Res*, 50, 806–  
465 822, <https://doi.org/10.1002/2013WR013604>, 2014.
- 466 Chiasson-Poirier, G., Franssen, J., Lafrenière, M. J., Fortier, D., and Lamoureux, S. F.: Seasonal  
467 evolution of active layer thaw depth and hillslope-stream connectivity in a permafrost  
468 watershed, *Water Resour Res*, 56, e2019WR025828,  
469 <https://doi.org/https://doi.org/10.1029/2019WR025828>, 2020.
- 470 Cooper, M. G., Zhou, T., Bennett, K. E., Bolton, R., Coon, E., Fleming, S. W., Rowland, J. C.,  
471 and Schwenk, J.: Detecting permafrost active layer thickness change from nonlinear baseflow  
472 recession, *Earth and Space Science Open Archive*, 48,  
473 <https://doi.org/10.1002/essoar.10511865.1>, 2022.
- 474 Curran, J. H. and Biles, F. E.: Identification of Seasonal Streamflow Regimes and Streamflow  
475 Drivers for Daily and Peak Flows in Alaska, *Water Resour Res*, 57, e2020WR028425,  
476 <https://doi.org/https://doi.org/10.1029/2020WR028425>, 2021.
- 477 Evans, S. G., Yokeley, B., Stephens, C., and Brewer, B.: Potential mechanistic causes of  
478 increased baseflow across northern Eurasia catchments underlain by permafrost, *Hydrol Process*,  
479 34, 2676–2690, <https://doi.org/https://doi.org/10.1002/hyp.13759>, 2020.



- 480 Frey, K. E. and McClelland, J. W.: Impacts of permafrost degradation on arctic river  
481 biogeochemistry, *Hydrol Process*, 23, 169–182, <https://doi.org/https://doi.org/10.1002/hyp.7196>,  
482 2009.
- 483 Hinzman, A., Sjöberg, Y., Lyon, S., Schaap, P., and van der Velde, Y.: Using a mechanistic  
484 model to explain the rising non-linearity in storage discharge relationships as the extent of  
485 permafrost decreases in Arctic catchments, *J Hydrol (Amst)*, 612, 128162,  
486 <https://doi.org/https://doi.org/10.1016/j.jhydrol.2022.128162>, 2022.
- 487 Hinzman, A. M., Sjöberg, Y., Lyon, S. W., Ploum, S. W., and van der Velde, Y.: Increasing  
488 non-linearity of the storage-discharge relationship in sub-Arctic catchments, *Hydrol Process*, 34,  
489 3894–3909, <https://doi.org/10.1002/hyp.13860>, 2020.
- 490 Jin, H., Huang, Y., Bense, V. F., Ma, Q., Marchenko, S. S., Shepelev, V. V., Hu, Y., Liang, S.,  
491 Spektor, V. V., and Jin, X.: Permafrost Degradation and Its Hydrogeological Impacts, *Water*  
492 (Basel), 14, 372, 2022.
- 493 Karlsen, R. H., Grabs, T., Bishop, K., Buffam, I., Laudon, H., and Seibert, J.: Landscape  
494 controls on spatiotemporal discharge variability in a boreal catchment, *Water Resour Res*, 52,  
495 6541–6556, <https://doi.org/10.1002/2016WR019186>, 2016.
- 496 Karlsen, R. H., Bishop, K., Grabs, T., Ottosson-Löfvenius, M., Laudon, H., and Seibert, J.: The  
497 role of landscape properties, storage and evapotranspiration on variability in streamflow  
498 recessions in a boreal catchment, *J Hydrol (Amst)*, 570, 315–328,  
499 <https://doi.org/10.1016/j.jhydrol.2018.12.065>, 2019.
- 500 Kirchner, J. W.: Catchments as simple dynamical systems: Catchment characterization, rainfall-  
501 runoff modeling, and doing hydrology backward, *Water Resour Res*, 45,  
502 <https://doi.org/10.1029/2008WR006912>, 2009.
- 503 Koch, J. C., Sjöberg, Y., O'Donnell, J. A., Carey, M. P., Sullivan, P. F., and Terskaia, A.:  
504 Sensitivity of headwater streamflow to thawing permafrost and vegetation change in a warming  
505 Arctic, *Environmental Research Letters*, 17, 44074, <https://doi.org/10.1088/1748-9326/ac5f2d>,  
506 2022.
- 507 Lamontagne-Hallé, P., McKenzie, J. M., Kurylyk, B. L., and Zipper, S. C.: Changing  
508 groundwater discharge dynamics in permafrost regions, *Environmental Research Letters*, 13,  
509 84017, <https://doi.org/10.1088/1748-9326/aad404>, 2018.
- 510 Lyon, S. W. and Destouni, G.: Changes in Catchment-Scale Recession Flow Properties in  
511 Response to Permafrost Thawing in the Yukon River Basin, *International Journal of*  
512 *Climatology*, 30, 2138–2145, <https://doi.org/10.1002/joc.1993>, 2010.
- 513 Lyon, S. W., Destouni, G., Giesler, R., Humborg, C., Mörth, M., Seibert, J., Karlsson, J., and  
514 Troch, P. A.: Estimation of permafrost thawing rates in a sub-arctic catchment using recession  
515 flow analysis, *Hydrol Earth Syst Sci*, 13, 595–604, <https://doi.org/10.5194/hess-13-595-2009>,  
516 2009.
- 517 Lyon, S. W., Mörth, M., Humborg, C., Giesler, R., and Destouni, G.: The relationship between  
518 subsurface hydrology and dissolved carbon fluxes for a sub-arctic catchment, *Hydrol Earth Syst*  
519 *Sci*, 14, 941–950, <https://doi.org/10.5194/hess-14-941-2010>, 2010.
- 520 Lyon, S. W., Nathanson, M., Spans, A., Grabs, T., Laudon, H., Temnerud, J., Bishop, K. H., and  
521 Seibert, J.: Specific discharge variability in a boreal landscape, *Water Resour Res*, 48,  
522 <https://doi.org/https://doi.org/10.1029/2011WR011073>, 2012.



- 523 Makarieva, O., Nesterova, N., Post, D. A., Sherstyukov, A., and Lebedeva, L.: Warming  
524 temperatures are impacting the hydrometeorological regime of Russian rivers in the zone of  
525 continuous permafrost, *Cryosphere*, 13, 1635–1659, <https://doi.org/10.5194/tc-13-1635-2019>,  
526 2019.
- 527 McKenzie, J. M., Kurylyk, B. L., Walvoord, M. A., Bense, V. F., Fortier, D., Spence, C., and  
528 Grenier, C.: Invited perspective: What lies beneath a changing Arctic?, *Cryosphere*, 15, 479–  
529 484, <https://doi.org/10.5194/tc-15-479-2021>, 2021a.
- 530 McKenzie, J. M., Kurylyk, B. L., Walvoord, M. A., Bense, V. F., Fortier, D., Spence, C., and  
531 Grenier, C.: Invited perspective: What lies beneath a changing Arctic?, *Cryosphere*, 15, 479–  
532 484, <https://doi.org/10.5194/tc-15-479-2021>, 2021b.
- 533 Muñoz Sabater, J.: ERA5-Land hourly data from 1981 to present,  
534 <https://doi.org/10.24381/cds.e2161bac>, 2019.
- 535 Muñoz Sabater, J.: ERA5-Land hourly data from 1950 to 1980,  
536 <https://doi.org/10.24381/cds.e2161bac>, 2021.
- 537 Obu, J., Westermann, S., Bartsch, A., Berdnikov, N., Christiansen, H. H., Dashtseren, A.,  
538 Delaloye, R., Elberling, B., Etzelmüller, B., Kholodov, A., Khomutov, A., Kääh, A., Leibman,  
539 M. O., Lewkowicz, A. G., Panda, S. K., Romanovsky, V., Way, R. G., Westergaard-Nielsen, A.,  
540 Wu, T., Yamkhin, J., and Zou, D.: Northern Hemisphere permafrost map based on TTOP  
541 modelling for 2000–2016 at 1 km<sup>2</sup> scale, *Earth Sci Rev*, 193, 299–316,  
542 <https://doi.org/10.1016/J.EARSCIREV.2019.04.023>, 2019.
- 543 Ploum, S. W., Lyon, S. W., Teuling, A. J., Laudon, H., and van der Velde, Y.: Soil frost effects  
544 on streamflow recessions in a subarctic catchment, *Hydrol Process*, 33, 1304–1316,  
545 <https://doi.org/10.1002/hyp.13401>, 2019.
- 546 Pöschlöd, B., Willkofer, F., and Ludwig, R.: Impact of Climate Change on the Hydrological  
547 Regimes in Bavaria, *Water (Basel)*, 12, <https://doi.org/10.3390/w12061599>, 2020.
- 548 Rantanen, M., Karpechko, A. Yu., Lipponen, A., Nordling, K., Hyvärinen, O., Ruosteenoja, K.,  
549 Vihma, T., and Laaksonen, A.: The Arctic has warmed nearly four times faster than the globe  
550 since 1979, *Commun Earth Environ*, 3, 168, <https://doi.org/10.1038/s43247-022-00498-3>, 2022.
- 551 Sergeant, F., Therrien, R., Oudin, L., Jost, A., and Anctil, F.: Evolution of Arctic rivers  
552 recession flow: Global assessment and data-based attribution analysis, *J Hydrol (Amst)*, 601,  
553 126577, <https://doi.org/10.1016/J.JHYDROL.2021.126577>, 2021.
- 554 Sjöberg, Y., Frampton, A., and Lyon, S. W.: Using streamflow characteristics to explore  
555 permafrost thawing in northern Swedish catchments, *Hydrogeol J*, 21, 121–131,  
556 <https://doi.org/10.1007/s10040-012-0932-5>, 2013.
- 557 Sjöberg, Y., Jan, A., Painter, S. L., Coon, E. T., Carey, M. P., O'Donnell, J. A., and Koch, J. C.:  
558 Permafrost Promotes Shallow Groundwater Flow and Warmer Headwater Streams, *Water  
559 Resour Res*, 57, e2020WR027463, <https://doi.org/https://doi.org/10.1029/2020WR027463>,  
560 2021.
- 561 Tananaev, N. and Lotsari, E.: Defrosting northern catchments: Fluvial effects of permafrost  
562 degradation, *Earth Sci Rev*, 228, 103996,  
563 <https://doi.org/https://doi.org/10.1016/j.earscirev.2022.103996>, 2022.
- 564 Troch, P. A., Berne, A., Bogaart, P. W., Harman, C., Hilberts, A. G. J., Lyon, S. W., Paniconi,  
565 C., Pauwels, V. R. N., Rupp, D. E., Selker, J. S., Teuling, A. J., Uijlenhoet, R., and Verhoest, N.



- 566 E. C.: The importance of hydraulic groundwater theory in catchment hydrology: The legacy of  
567 Wilfried Brutsaert and Jean-Yves Parlange, *Water Resour Res*, 49, 5099–5116,  
568 <https://doi.org/doi:10.1002/wrcr.20407>, 2013.
- 569 Walvoord, M. A. and Striegl, R. G.: Increased groundwater to stream discharge from permafrost  
570 thawing in the Yukon River basin: Potential impacts on lateral export of carbon and nitrogen,  
571 *Geophys Res Lett*, 34, L12402, <https://doi.org/10.1029/2007GL030216>, 2007a.
- 572 Walvoord, M. A. and Striegl, R. G.: Increased groundwater to stream discharge from permafrost  
573 thawing in the Yukon River basin: Potential impacts on lateral export of carbon and nitrogen,  
574 *Geophys Res Lett*, 34, <https://doi.org/10.1029/2007GL030216>, 2007b.
- 575 Walvoord, M. A., Voss, C. I., and Wellman, T. P.: Influence of permafrost distribution on  
576 groundwater flow in the context of climate-driven permafrost thaw: Example from Yukon Flats  
577 Basin, Alaska, United States, *Water Resour Res*, 48, <https://doi.org/10.1029/2011WR011595>,  
578 2012.
- 579 Walvoord, M. A., Voss, C. I., Ebel, B. A., and Minsley, B. J.: Development of perennial thaw  
580 zones in boreal hillslopes enhances potential mobilization of permafrost carbon, *Environmental*  
581 *Research Letters*, 14, 15003, <https://doi.org/10.1088/1748-9326/aaf0cc>, 2019.
- 582 Wang, J., Chen, X., Gao, M., Hu, Q., and Liu, J.: Changes in nonlinearity and stability of  
583 streamflow recession characteristics under climate warming in a large glaciated basin of the  
584 Tibetan Plateau, *Hydrol Earth Syst Sci*, 26, 3901–3920, [https://doi.org/10.5194/hess-26-3901-](https://doi.org/10.5194/hess-26-3901-2022)  
585 2022, 2022.
- 586 Wang, K., Zhang, T., and Yang, D.: Permafrost dynamics and their hydrologic impacts over the  
587 Russian Arctic drainage basin, *Advances in Climate Change Research*, 12, 482–498,  
588 <https://doi.org/10.1016/J.ACCRE.2021.03.014>, 2021.
- 589 Wang, Q., Qi, J., Wu, H., Zeng, Y., Shui, W., Zeng, J., and Zhang, X.: Freeze-Thaw cycle  
590 representation alters response of watershed hydrology to future climate change, *Catena (Amst)*,  
591 195, 104767, <https://doi.org/https://doi.org/10.1016/j.catena.2020.104767>, 2020.
- 592 Wellman, T. P., Voss, C. I., and Walvoord, M. A.: Impacts of climate, lake size, and supra- and  
593 sub-permafrost groundwater flow on lake-talik evolution, Yukon Flats, Alaska (USA),  
594 *Hydrogeol J*, 21, 281–298, <https://doi.org/10.1007/s10040-012-0941-4>, 2013.
- 595